Geometry and topology of Polish Outer Carpathian digital elevation model interpreted lineament network in context of regional tectonics

Maciej Kania[1], Mateusz Szczęch[1]

[1]Jagiellonian University in Kraków, Faculty of Geography and Geology, Institute of Geological Sciences, Gronostajowa 3a, 30-863 Kraków, Poland

Correspondence to: Maciej Kania (maciej.kania@uj.edu.pl)

Abstract. The Polish part of the Western Outer Carpathians lineament network was analysed based on the GMTED2010 digital elevation model. Lineaments were identified in the visual screening of the hillshade model. To the best of our knowledge, no one has studied the geometrical properties of the network with relation to the topological ones. The NetworkGT QGIS toolbox was applied to identify the nodes and branches of the network, as well as to calculate the topology parameters. Our aim was to find differences between the western and eastern parts of the Western Outer Carpathians; therefore, the analyses were carried out in six sectors chosen based on the geographical subdivision in the geological context: three in the north, mainly the Silesian unit; and three in the south, mainly the Magura unit. We found general agreement of the identified network with the photolineament map; however, some of the photolineaments are not confirmed by digital elevation model (DEM). We found that the topological parameters of the networks change from west to east, but not from north to south. There are areas of increased interconnectivity, especially the Nowy Sącz Basin, where the lineament network may reflect a complicated system of cross-cutting deep-rooted fault zones in the basement.

1. Introduction

Remote sensing imagery is an important source of data in regional tectonics, and its importance has been growing in recent years. Since the 1970s, there have been multispectral satellite photos of the Earth surface applied mainly in mineral mapping (e.g. van der Meer et al., 2012), as well as in tectonic studies (e.g. Leech et al., 2003). The Shuttle Radar Topography Mission (SRTM) resulted in the first remote sensing digital elevation model of most of the continental surface of the planet, with immense potential for application in geology (Yang et al., 2011). Then, new superior resolution and quality models were created on both the global (satellite) and local scale (mainly airborne LiDAR scanning). Digital elevation models are especially useful in areas with lush vegetation. The application of LiDAR in the Carpathians' flysch-type mountains in geological interpretations was shown, for example, in Kania and Szczęch (2022).

Our previous study (Kania and Szczęch, 2020), based on the interpretation of the model augmented with field geological mapping (Szczęch and Cieszkowski, 2021), showed how a lineament network can be interpreted in topological and geometrical terms. The aim in the present paper is to up-scale DEM-based geometrical and topological analyses of a regional scale lineament network to find how this is reflected in the tectonic structure of the Western Carpathians. Previous studies of the Carpathian lineaments were mainly focused on lineament strikes distribution (e.g. Doktór and Graniczny, 1982, 1983; Doktór et al., 1985, 1990, 2002; Bażyński et al., 1986; Graniczny and Mizerski, 2003)**;** therefore, we decided to add an interconnectivity aspect in terms of the topological parameters (Valentini et al., 2007; Sanderson and Nixon, 2015; Thiele et al., 2016), as a way of better understanding the structural problems. Most of the Carpathian-related studies are geographically organised in mountain arc parallel belts, reflecting the main tectonostratigraphic units, now forming nappes and being sedimentary basins during the Carpathian flysch depositions. We decided to keep this subdivision, although combining this with physiographical subdivisions into sectors with borders perpendicular to the Carpathian belt.

2. Up-to-date research on the Polish Outer Carpathian lineaments

The fact that dislocation lines perpendicular to the Carpathian arc are related to the deep basement, and are significantly older than the Carpathians themselves, was postulated even before the remote sensing era (Teisseyre, 1907). The first modern attempts to interpret lineaments in the Polish Carpathians were based on the Landsat MSS imagery and Heat Capacity Mapping Mission satellite, and reported together with data from the

whole territory of Poland on a photogeological map at 1:1 000 000 scale (; Bażyński et al., 1986; Graniczny and Mizerski, 2003). The main lineament systems of the Western Carpathians in the context of structural geology were shown by Doktór and Graniczny (1983) and Doktór et al. (1985). The results of satellite imagery lineament detections were then correlated with geophysical data proving relationships between the surface, neotectonic processes and deep Carpathian basement structure (Motyl-Rakowska and Ślączka, 1984; Doktór et al., 1990). Airborne radar data were applied in tectonic analysis of the Carpathians, resulting in 17 000 short lineaments that were the basis of the lineament density map (Doktór et al., 2002). The interpretation of SRTM hillshading visualisation was performed by Chodyń (2004) on the limited area in Beskid Wyspowy Mts. Comparison of Landsat MSS and SRTM data by Ozimkowski (2008) showed that whilst the main faults can be related to lineaments, there are still numerous lineaments without geological explanation.

3. Study area

The choice of the study area was based on the physiogeographical subdivision of Poland by Solon et al. (2018). The following macroregions were selected: the Western Beskidy Foothills, Western Beskidy Mts., Orawa–Podhale Basin, Mid-Beskidy Foothills and Mid-Beskidy Mts (Fig. 1). These five regions, with a total area of 17 437 km^2, cover most of the Polish part of the Outer Carpathians, excluding a small part of the Eastern Outer Carpathians located in Poland.

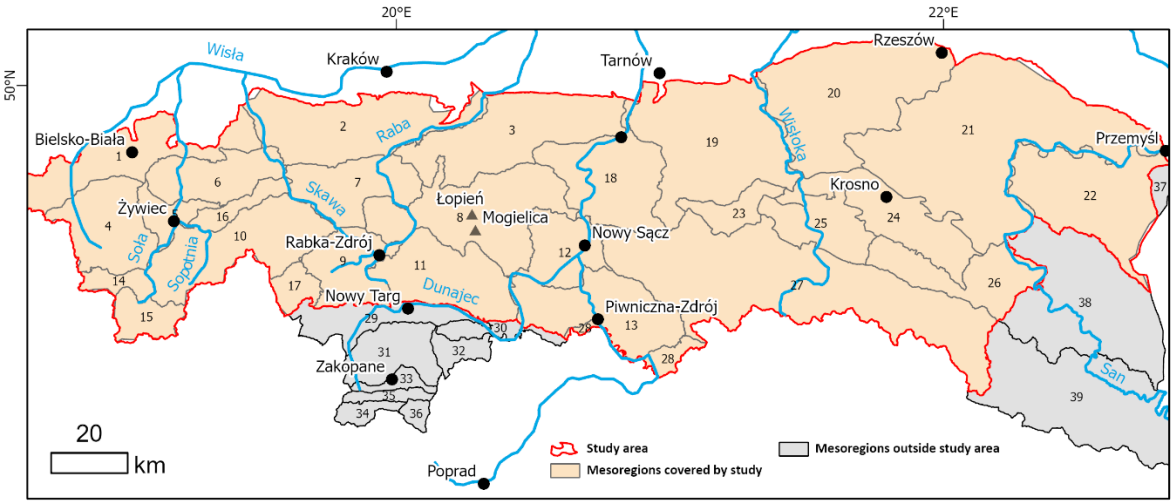

Fig. 1. Physiogeographical subdivision of the study area and adjancted parts of the Polish Carpathians based on Solon et al. (2018). Mesoregions covered by study: 1 – Silesia Foothills, 2 – Wieliczka Foothills, 3 – Wiśnicz Foothills, 4 – Silesian Beskid Mts, 5 – Żywiec Basin, 6 – Mały Beskid Mts, 7 – Makowski Beskid, 8 – Wyspowy Beskid, 9 – Orawa-Jordanów Foothills, 10 – Żywiec-Orawa Beskid Mts, 11 – Gorce Mts, 12 – Sącz Basin, 13 – Sącz Beskid Mts, 14 – Koniaków Intermontane Region, 15 – Żywiec-Kysuce Beskid Mts, 16 – Pewel-Krzeczów Ranges, 17 – Orawa Interfluve, 18 – Rożnów Foothills, 19 – Ciężkowice Foothills, 20 – Strzyżów Foothills, 21 – Dynów Foothills, 22 – Przemyśl Foothills, 23 – Gorlice Basin, 24 – Jasło-Krosno Basin, 25 – Jasło Foothills, 26 – Bukowiec Foothills, 27 – Low Beskid Mts, 28 – Poprad Foothills; mesoregions outside the study area: 29 – Orawa-Nowy Targ Basin, 30 – Pieniny Mts, 31 – Fore-Tatra Foothills, 32 – Magura Spiska Mts, 33 – Sub-Tatra Depression, 34 – Western Tatra Mts, 35 –

Reglowe Tatra Mts, 36 – High Tatra Mts, 37 – Hermanowice Submontane Region, 38 – Sanocko-Turczańskie Mts, 39 – Bieszczady Mts.

3.1 Geological setting of the study area

The research area is located in the Polish sector of the Western Outer Carpathians (Mahel', 1974; Książkiewicz, 1977; Ślączka et al., 2006; Fig. 2). It contacts tectonically with the Pieniny Klippen Belt from the south, which is a border between the Outer and the Central Carpathians (Książkiewicz, 1977; Plašienka, 2018; Golonka et al., 2019, 2021). The basement under the Western Outer Carpathians is formed of two blocks: Brunovistulicum and Małopolska Massif, which are separated by major tectonic zone: Kraków – Lubliniec Fault (Fig. 2B) Żaba, 1999; Żelaźniewicz, 2011), cut by numerous other deep rooted lineaments (Doktór, 1985). The Outer Carpathians are built mainly of flysch deposits, whose thickness is approximately 6 000 m, and thus they are also referred to as the Flysch Carpathians (Książkiewicz, 1977; Golonka et al., 2005, 2021; Ślączka et al., 2006;. These deposits are Late Jurassic–Early Miocene in age and are mainly deep-sea sediments deposited by the gravity flow in the several sedimentary basins of the Northern Tethys, separated by ridges (Książkiewicz, 1977; Golonka et al., 2005, 2021; Ślączka et al., 2006). The thrust of the Central Carpathians block to the north on the European Platform blocks — the Brunovistulicum and Małopolska Massif (Żaba, 1999) — led to the forming of the synorogenic stage accretionary prism. The sediments deposited in the basins were folded and thrusted one upon another, creating the sequence of the nappes in the Miocene. Going from the south there are the Magura Nappe, Dukla Nappe, Fore–Magura group of nappes, Silesian Nappe, Sub-Silesian Nappe and Skole Nappe (Mahel', 1974; Książkiewicz, 1977; Golonka et al., 2005, 2019; Ślączka et al., 2006). The deposits of the Outer Carpathians are overthrust on the Miocene molasses filling the Carpathian Foredeep, which was deposited on the front of the Outer Carpathian orogenic belt thrusting over the North European Platform (Ślączka et al., 2006; Oszczypko, 2006).

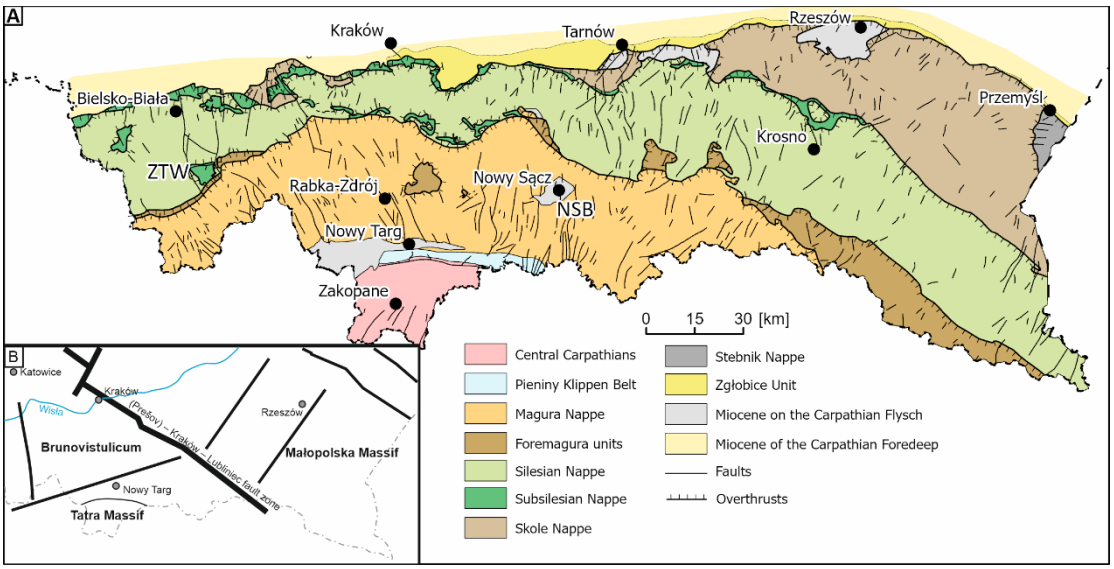

Fig. 2. A: Generalised geological map of the Polish part of the Carpathians based on Cieszkowski et al., 2017 and cited there, faults after Lexa et al., 2000. B: .Main tectonic units under the Carpathians, after Żelaźniewicz et al., 2011.

3.2 Analysis of the sectors

We used the morphometry subdivision of Poland (Solon et al., 2018) to define the area, based on the subprovinces of the Western Outer Carpathians in the area of Poland and a small band of Northern Subcarpathia subprovince to the border of the Carpathians in the geological meaning (Carpathian overthrust on the Foredeep sediments), according to Lexa et al. (2000). The subdivision of the outer Carpathian belt is mostly used in the geology basis on the tectonostratigraphic units (nappes). This subdivision, however, does not allow differences in lineament systems parallel to the belt to be caught. The newly proposed morphostructural subdivision of the Western Carpathians (Minár et al., 2011) is another approach that compiles geological and morphological features. The Polish part of the Western Carpathians is subdivided into the following subregions (number according to the paper cited): (3f) Moravian–Silesian Beskid, (3a) Beskid Żywiecki–Gorce, (3b) Beskid Sądecki–Levočské vrchy, (5a) Beskid Wyspowy, (5b) Low Beskid and (6) North Foreland. The last subregion spans all the length of the northern Carpathian boundary between the Orava and San rivers. We decided to compile the geological subdivision with the morphological one (Solon et al., 2018), which also comprises a subdivision of the outermost units, into five sectors (Fig. 3, Tab. 1). The only change was including Mount Ciecień in Beskid Wyspowy into the Central Silesian sectors, as this massif, unlike all other Beskid Wyspowy culminations is built of Silesian series deposits (Burtan, 1974).

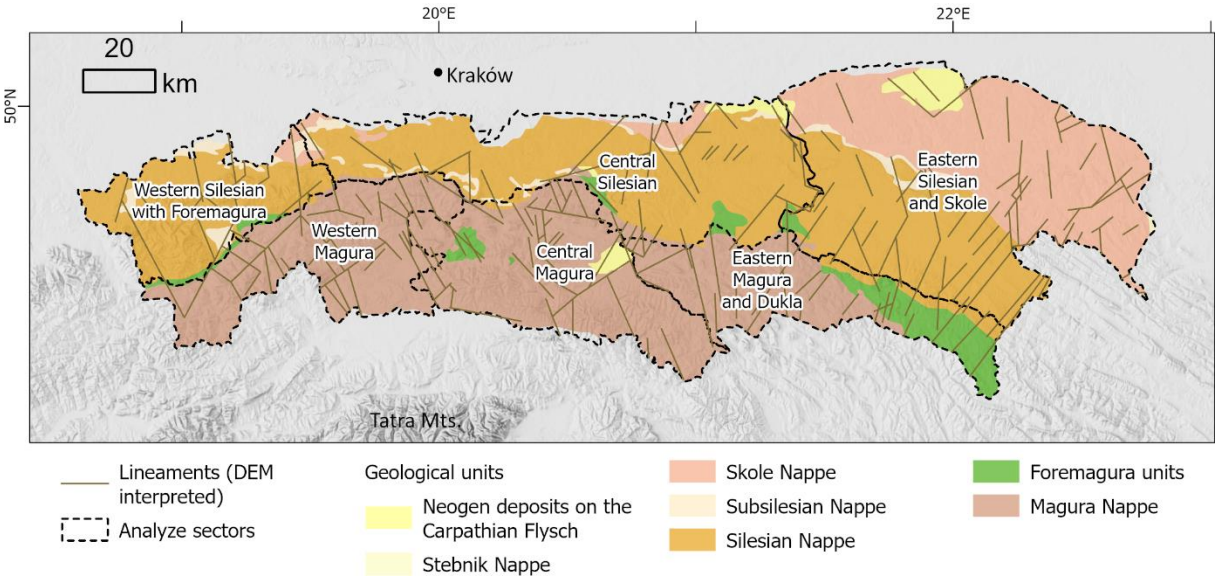

Fig. 3. Sectors defined based on the physiogeographical (Solon et al., 2018) and tectonic subdivisions (Golonka et al., 2021) of the study area (Western Outer Carpathians in Poland).

Tab. 1. Analyse sectors

Analyse sectors name;	**Symbol**	**Mesoregions covered according to** Solon et al., 2018
Western Silesian with Foremagura	WS	Silesian Beskid Mts., Żywiec Basin, Silesia Foothils, Mały Beskid Mts.
Central Silesian	CS	Wieliczka Foothils, Wiśnicz Foothils, Beskid Wyspowy Mts – only the Ciecień ridge, Rożnów Foothils, Ciężkowice Foothils, Gorlice Basin

Eastern Silesian and Skole	ES	Przemyśl Foothils, Jasło-Krosno Basin, Strzyżów Foothills, Dynów Foothils, Jasło Foothils, Bukowiec Foothills
Western Magura	WM	Orawa-Jordanów Foothills, Orawa Interfluve, Koniaków Intermontane Region, Żywiec-Kysuce Beski, Pewel-Krzeczów Ranges, Makowski Beskid, Żywiec-Orawa Beskid
Central Magura	CM	Sącz Beskid Mts., Sącz Basin, Wyspowy Beskid (without Ciecień Ridge), Gorce Mts.
Eastern Magura and Dukla	EM	Low Beskid Mts.

4. Digital elevation model

The Global Multi-resolution Terrain Elevation Data 2010 (GMTED2010; see Danielson, 2011) 7.5 arc-second product was chosen as a work base. The model is a compilation of different raster-based elevation sources, based mainly on SRTM digital terrain elevation data. The resolution is ca. 0.0021°/pixel, which means ca. 233 m/pixel. This was found to be sufficient, while the working scale during lineament detection was 1:150 000. As the shading azimuth can influence the results, the working imagery was multidirectional hillshade (Nagi, 2022.

5. Methods

5.1 Multiple cover lineament detection

The manual method of lineament extraction was applied for two reasons. First, it is the simplest, low cost and widely used method. The second reason is that it creates a basis for further work, based on automated extraction. However, the method used is prone to some operator-related bias (Scheiber et al., 2015; Ehlen, 2004). Thus, to reduce this bias the lineaments were extracted by two operators working independently, in three sessions, separated by intervals of several months. After each session, the results were analysed and a network of common features was created. Lineaments marked by both operators were merged into single feature. Lineaments marked by only one operator were removed. The last stage was creating a concise network of lineaments based on the results of the three sessions.

5.2 Network analysis

A network can be described by scale-independent topological characteristics, based on the case of a line network on graph theory. The network (graph) is formed by nodes (end or intersection points) connected by lines (Sanderson and Nixon, 2015; Mukherjee, 2019). The line can be formed by one or more branches connected by nodes. The node can be isolated (I type), an embranchment (Y type) or an intersection (X type), where the latter two types are connecting nodes. Thus, the branch can connect two I type nodes (I–I branch), isolated and connecting nodes (I–C branch, which can be I–Y or I–X) and two connecting nodes (C–C branch, which can be X–X, X–Y or Y–Y). The proportion of nodes and branch types can be analysed as tertiary systems that

characterise the properties of the network, especially its interconnectivity (Procter and Sanderson, 2018; Sanderson and Nixon, 2015; Sanderson et al., 2018).

The spatial variation of the topological parameters of the network was analysed with the following aspects: (1) regular, in a 5x5 km grid; and (2) within sectors based on the mesoregions of physiogeographical subdivision, according to Solon et al. (2018) and the main tectonic units (Fig. 3 Tab. 1).

The NetworkGT Qgis toolbox (Nyberg et al., 2018) was used as a tool in the topological analyses. The lineament network was checked and repaired with NetworkGT tools. An additional stage was the manual correction of some features to eliminate all non-defined types of nodes, as well as some extremely short (ca. 500 m or shorter) features. The topological parameters were analysed in three modes: the whole network; the sectors defined; and in a regular, 5x5 km grid with 10 km search radius.

The Rayleigh test of semicircular distribution test was performed with the EZ-ROSE spreadsheet (Baas, 2000), and circular statistics were calculated with the SciPy stats module (The SciPy Community, 2022).

6. Results

6.1 Network geometry

The azimuths of the lineaments in all the analysed sectors show a multimodal distribution. Thus, the directions were separated into sets, in a way that gives low values of circular variance. The angular ranges of all the sets are presented in Tab. 2. For all sets, except for set 2 in the Eastern Magura (EM) sector and set 2 in the Western Silesian (WS) sector, the distribution is not uniform, as checked with the Rayleigh test (Baas, 2000). The two sets not checked were not numerous enough to be representative.

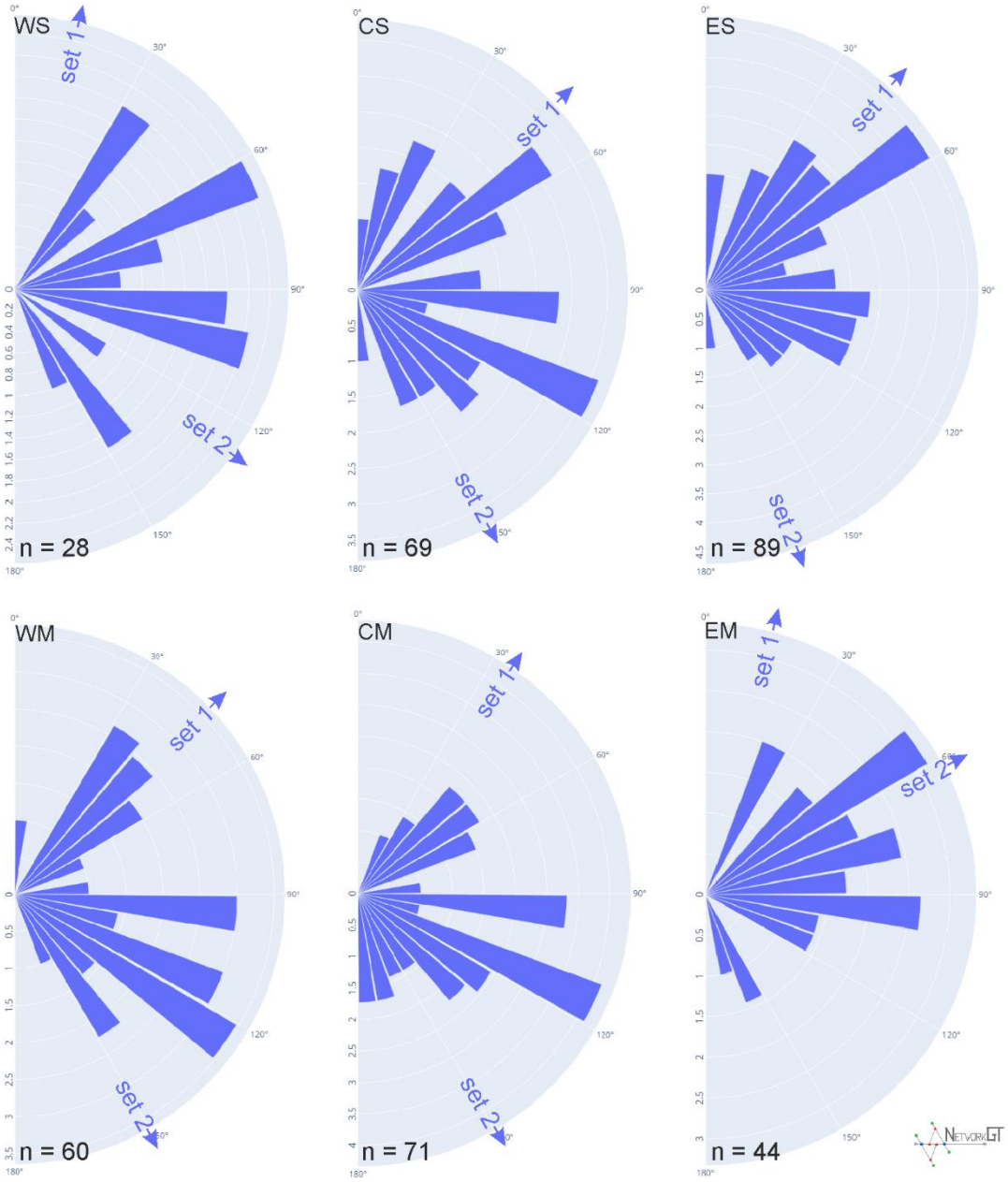

Fig. 4: Rose diagrams of the analysed networks in the analytic sectors; upper row: Western Silesian sector with Foremagura (WS), Central Silesia (CS), Eastern Silesia with Skole (ES); lower row: Western Magura (WM), Central Magura (CM), and Eastern Magura with Dukla (EM). Arrows mark the mean azimuth for the sets defined in Tab. 2.

Tab. 2. Azimuths of the lineaments in the analyse sectors

Analyse sector	Set	Azimuths range	n	Circular statistics			The acute angle between sets means
				Mean	Std. dev	Variance	
CS	1	0 – 100	15	46.5	14.2	3.5	75.5
	2	100 – 180	13	151	16.6	4.8	

CM	1	0 – 80	17	34.1	13	3	63.9
	2	80 – 180	51	150.2	21.5	8.1	
EM	1	45 – 75	41	62.1	7.5	1.0	47.7
	2	0 – 45 75 – 180	3	14.4	26.7	12.5	
ES	1	0 – 100	59	42.7	19.7	6.8	62.1
	2	100 – 180	28	160.6	14.7	3.8	
WM	1	0 – 100	20	46.5	14.2	3.5	75.5
	2	100 – 180	40	151	16.6	4.8	
WS	1	0 – 60 150 – 180	23	13.6	23.3	9.5	66.2
	2	60 – 150	5	127.4	8.9	1.4	

The orientation of lineaments in all sectors, as well as the circular mean azimuth are shown in Fig. 4. In sectors Central and Eastern Silesian (CS, ES) and Central and Western Magura (CM, WM) the set 1 mean is located between 34° and 47°, marking a dominant SW–NE strike of lineaments. In the Western Silesian sector (WS), set 1 is oriented more to the north (14°). In all sectors above, there is a second set with a NW–SE trend, mostly oriented at 150–160°, but in the Western Silesian sector case the mean azimuth is lower (127°), as in the case of the first set. The last sector, Eastern Magura and Dukla, is different. There is one dominant set with azimuth 62°, and the second set is poorly represented and oriented northward. The angle between the two sets varies in the 62–76° range, except in the Eastern Magura and Dukla sector where it is only 48°.

6.2 Network topology

In the study area, 305 lineaments were marked in total. These features comprise 432 nodes. Of this count, 58% are I nodes, 19% are E nodes, 18% are Y nodes and 5% are X nodes. The network contains 338 branches, within which 49% are C–I type branches, 29% are C–C branches and 22% are I–I branches marking completely separated lineaments. Topological parameters are shown in Tab. 3.

Tab. 3. Topological parameters of the network in analyse sectors

	Western Silesian with Foremagura	**Central Silesian**	**Eastern Silesian and Skole**	**Western Magura**	**Central Magura**	**Eastern Magura and Dukla**	**Whole area**
	WS	**CS**	**ES**	**WM**	**CM**	**EM**	
No. of nodes (I+X+Y)	19	68	101	47	67	40	383
I nodes	8	51	76	26	48	36	293
X nodes	1	6	6	3	6	2	19
Y nodes	10	11	21	18	15	2	71
E nodes	22	38	49	46	61	52	-

C-C connections	11.5	14.5	18.5	21.0	33.5	3.0	77.0
C-I connections	8.5	28.5	35.5	22.0	25.0	11.5	131.0
I-I connections	1.0	11.0	23.5	3.0	14.0	10.5	81.0
No. of branches	21.0	54.0	77.5	46.0	54.5	25.0	291
No. of lines	9.0	31.0	48.5	22.0	31.5	19.0	182
No. of connections	11	17	25	21	19	4	90
Connects per line	2.44	1.10	1.03	1.91	1.21	0.42	0.99
Connects per branch	1.62	1.06	1.02	1.43	1.12	0.56	0.99
Dim.less intensity	1.21	0.87	1.21	1.65	1.33	2.06	0.75
Av. Degree of network	2.21	1.59	1.53	1.96	1.63	1.25	1.52

The highest dimensionless intensity parameter is in the Eastern Magura and Dukla sector (2.05) and the lowest in the Central Silesian (0.87). On the other hand, the Eastern Magura sector is characterised by the lowest connections per branch (0.56) or the average degree of network (1.25) due to its form of mainly parallel features, with only 12% of the branches of connecting type (C–C). The best interconnectivity is observed in the Western Silesian sector with 1.62 connections per branch and an average degree of the network of 2.21. This is an effect of the presence of the Żywiec Basin block-system in the central part of the region.

The difference between these two (Eastern Magura and Western Silesia) sectors can be clearly visible on the ternary diagrams (Fig. 5) presenting the relationships of the nodes and branch types. In the Western Silesian sector, there is a high ratio of Y type nodes (52% of non-E-type nodes) and only one I–I branch.

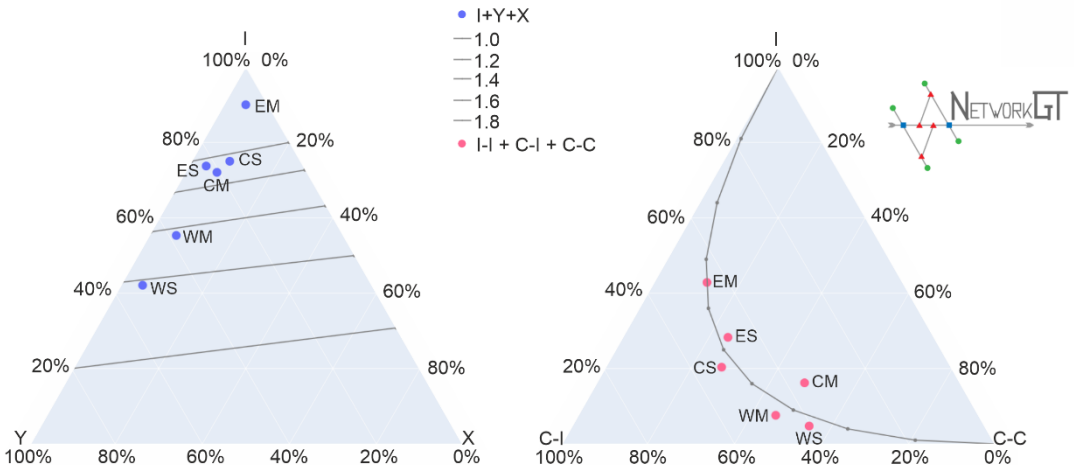

Fig. 5: Ternary diagram presenting nodes (left) and branches (right) proportions in the analyse sectors.

The parameters of all the other sectors fall between the Eastern Magura and Western Silesian sectors. The Western Magura sector has quite good interconnectivity with a similar type of Eastern Magura blocky network.

Another approach to analysing topology is to use a sampling regular grid. The results are shown in Fig. 5 as maps of connections per branch number, 2D network intensity and dimensionless intensity.

It can be seen we have two relatively large regions with a high value of connections per branch parameter . The first one is in the Western Silesian and partially Western Magura sectors, that is, the Żywiec Basin area, but from the geological point of view it is also a narrow zone of Foremagura units occurring between the Silesian and Magura nappes. Moreover, the Subsilesian unit tectonic window occurs in this area.

The Nowy Sącz Basin (eastern part of the Central Magura sector in the subdivision used here) is the next region with a high number of connections per network branch. The lineament system in this area surrounds a zone of Neogene deposits lying on the Carpathian flysch and filling the intramountain Nowy Sącz Basin.

The 2D intensity map shows that the Nowy Sącz Basin is characterised in general by a higher intensity than the Żywiec Basin. There is also a general trend of higher intensity in the western part of the Carpathians (especially the Western Magura and Central Magura sectors) than in the eastern part (Eastern Magura and Dukla).

In terms of dimensionless intensity parameter there are two regions with significantly high values: the south-eastern part of the Wiśnicz foothill, which is in the Central Silesian sector, and the eastern parts of the Beskid Niski Mts. and Bukowiec foothill in the Eastern Magura and Eastern Silesian sectors, on the geographical border of the Western and Eastern Carpathians.

7. Discussion

7.1 Different lineament identification approaches

There are 110 photolineaments marked on the photogeological map of Poland in the studied area (Bażyński et al., 1986). In the same area of the geological map of the Carpathians, Lexa et al. (2000) marked 2 325 features described as a fault or assumed fault. In many cases, our lineament system seems to be concordant or complimentary to Lexa et al.'s (Fig. 6). In some cases, the features marked as faults are rather thrust lines, as per the Fig. 6a example. The photolineament system is in general concordant with the DEM-interpreted system.

Visual inspection of the compiled lineaments map (Fig. 7a) shows that the especially NE striking lineaments of

the Eastern Magura sector are consistent with each other. Moreover, the system framing the Żywiec tectonic window is well visible in both sets. On the other hand, there are some photolineaments that are not recognisable on the DEM, and in fact also hardly visible on the modern orthophoto map. The most prominent example are two straight, parallel lineaments striking the NNE in the central part of the study area, cutting its entire width. These features seem to cut Gorce Mts.; this is not confirmed by our other studies (Kania and Szczęch, 2020; Szczęch and Cieszkowski, 2021). Further to the north, these two lineaments are delimiting massifs of the Beskid Wyspowy Mts. (Mogielica, Łopień). These massifs are in fact particularly visible on the aerial photo, as rather isometric 'islands', and are formed by core parts of the synclines (Wójcik et al., 2009). On the other hand, some lineament systems well visible in DEM are not marked on the photolineament map, as per the case of the system north of the Nowy Sącz. That shows how these two methods can in fact be recognised as complementary approaches to the lineaments' identification.

The system from the map by Lexa et al. (2000) shows confirmed and inferred faults, which is why it is not fully compatible with lineaments; the lineaments, even when mainly tectonic related, are in fact a broader term (O'Leary et al., 1976). Especially, these data, despite being a very rich collection of features are not applicable for topological analyses: most of the features are short and isolated even when forming a network. Nevertheless, these data include faults that are identified with geological criteria that are not visible in the remote sensing (at least at the scale applied in this paper or by Bażyński et al., 1986 photolineament map. These data are augmenting each other, which is highly visible in the Piwniczna Zdrój area, where DEM interpreted that the NNW striking lineament along the Poprad River Valley (not present in the photolineament set) is flanked with a set of N or NNE striking faults, which we have not identified on the DEM.

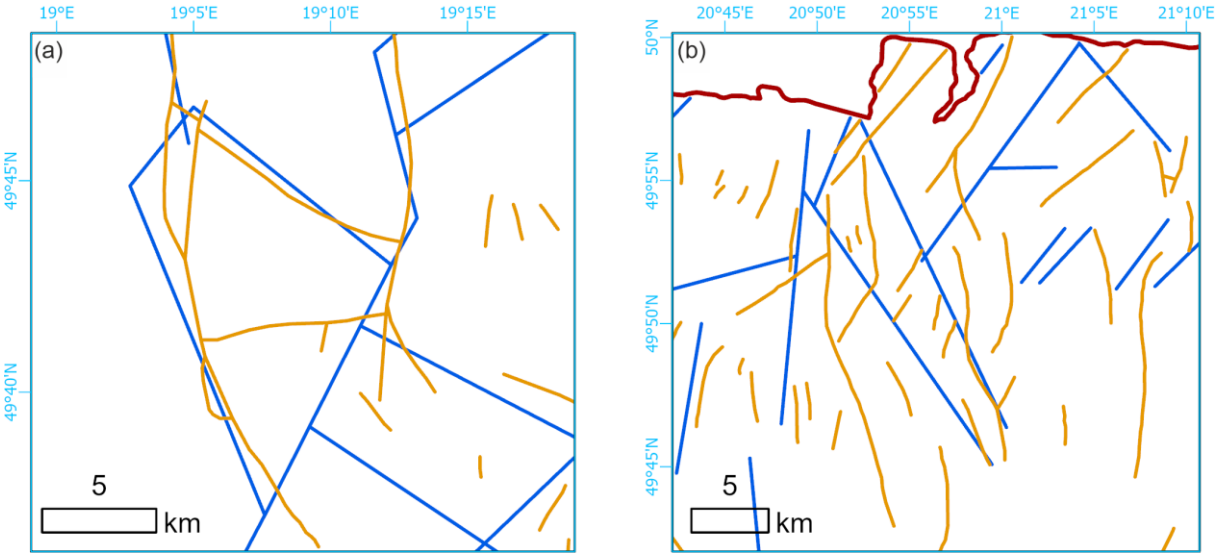

Fig. 6. Comparison of lineament system detected from the GMETD model (blue) and faults by Lexa et al., 2000 (brown). (a) Żywiec Basin area, (b) fragment of the Zakliczyn – Olszyny fault zone.

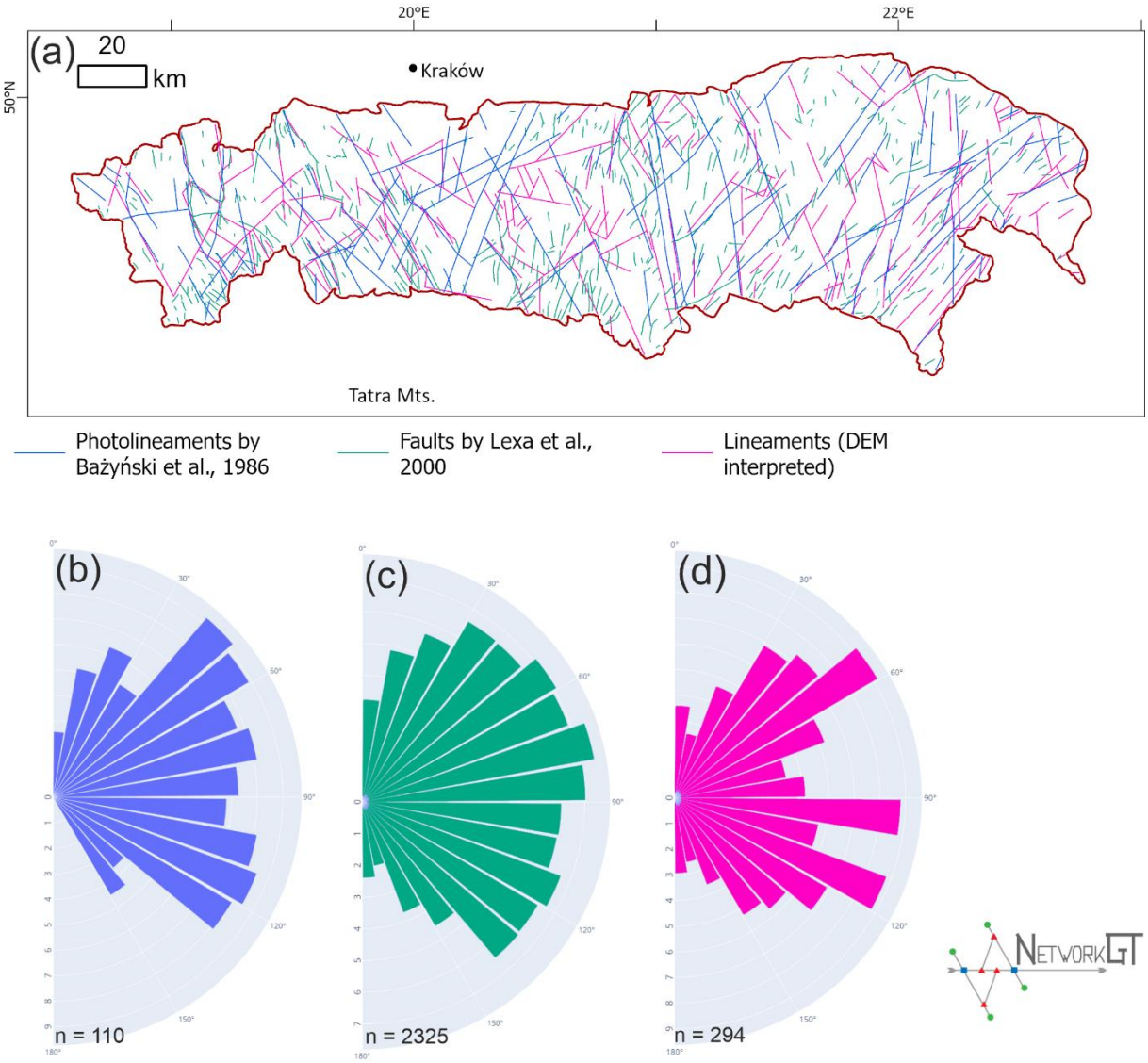

Fig. 7. Geometry of lineament networks in the Carpathians. (a) compilation map of lineaments by Bażyński et al., 1986, faults by Lexa et al., 2000 and lineaments interpreted from DEM in the presented paper. (b-d) rosediagrams of features azimuth in the whole study area from: (b) Bażyński et al. (1986), (c) Lexa et al., 2000 and (d) DEM interpreted.

When analysing the distribution of feature azimuth for the whole study area (Fig. 7b-d), it can be noted that the directions for the photolineament set (B) and DEM-interpreted set (D) are quite similar. What is noteworthy is the lack of azimuths greater than 150° in the photo set, which are present (albeit in a minority) in the DEM set. Furthermore, the photo set shows two maxima, at ca. 45° and 110°, whilst in the DEM set there are three maxima at ca. 50°, 100° and 110°. However, the dominating directions are not in fact distributed uniformly along the W–E span of the Polish Western Carpathians, which can be clearly seen in Fig. 7a where the domination of NE directions in the eastern sectors can be noticed, as well as the presence of two main directions in the western and central sectors.

7.2 Dominating directions of the lineament network

We observed a difference in dominating azimuths of lineaments between the western/central sectors (WS, WM, CS, CM) and eastern sectors (ES, EM) of the study area. The first ones are characterised by two distinct sets of lineaments (NNE or NE and SE), while the second has an SE set that is strongly reduced.

According to the general tectonic model of the Outer Carpathians (Unrug, 1980), the flysch deposits are cut by set sinistral strike–slip fault zones. These fault zones are arranged in a fan-like shape along the arc of the Carpathians, leading to the rotation of the set of nappes (Unrug, 1980; Graniczny and Mizerski, 2003). The observed trend of increasing importance of the NE direction to the east is consistent with this model. However, the more complicated geometry of the western part of the network may be related to the more complicated system of the deep-rooted fault zones in this part (see further discussion below).

7.3 Topological differentiation of the network

There are no topological analyses of the lineament networks for the Outer Carpathians. Our previous article (Kania and Szczęch, 2022) was focused on one mountain massif: Gorce Mts. From the tectonic point of view, this massif is quite homogenous, being located in the one tectono-facial unit (Magura unit) with some subunits within (Bystrica and Krynica subunits). Therefore, the paper focused mainly on different litostratigraphic units, showing how different types of lithology differ in topology terms.

Scaling the research into the Polish Western Carpathians shows that in general there are no differences in the network topology related to the tectono-facial units (Outer Carpathian nappes) since in general, all these units are similar in lithology (flysh packets). However, there are differences related to some irregularities in tectonics: especially, the intramountain basins are marked with increased network interconnectivity. The western part of the study area in general has a better developed network. Especially, the Eastern Magura differs from the rest of the sectors: the domination of one lineament direction results in low network interconnectivity, which is expressed by a high proportion of the I nodes and I–I branches (Fig. 5). We analysed Magura unit and part of the Dukla unit together; however, the interconnectivity in the Dukla Nappe (belonging to the Foremagura group) is stronger than in Magura, which can be related to the proximity of the Silesian unit overthrust.

The highest interconnectivity was observed in the Western Silesian sector. The area is characterised by a high proportion of Y nodes, and thus mainly by the presence of C–I or C–C branches (Fig. 5). In the geological context, it is related to the location of the Żywiec tectonic window, which exposes the Subsilesian unit. However, the topological study shows that the tectonised zone is wider; the increase in connections per branch zone continues to the south along the Soła River and further, at least to the state border in the Beskid Żywiecki Mts.

7.4 Main large-scale, deep-rooted lineament systems of the Western Carpathians and their relation to DEM-interpreted lineaments

The following, well-known, large-scale lineaments reach the Carpathian basement cutting the Polish part of the Outer Western Carpathians (Doktór et al., 1985): Central Slovakia, Myjava, Muran, Štitnik and Przemyśl. There are also lineaments not named by Doktór et al. (1985), but striking parallel, approximately 10 km to the east from the Skawa fault zone (Cieszkowski et al., 2006). Fig. 8 presents the generalised positions of the lineaments.

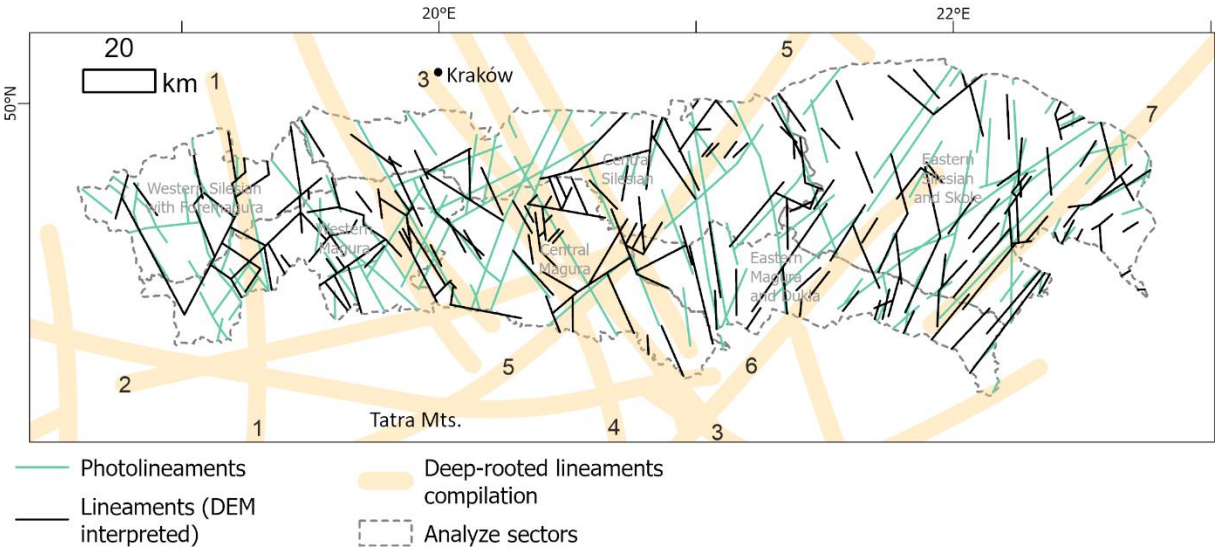

Fig. 8. Interpreted lineament system with photolineaments by Bażyński et al., 1986 as well as deep-rooted lineament compilation after Sikora, 1976; Zuchiewicz, 1984; Doktór et al., 1985. Important deep-rooted lineaments mark with numbers: 1 – Central Slovakia, 2 – Pericarpathian, 3 – Kraków – Prešov, 4 – Stitnik, 5 – Myjava, 6 – Muran, 7 - Przemyśl

The central Slovak line marks the eastern border of the Żywiec basin and marks the major fault zone well visible in the displacing Fore–Magura belt near Żywiec. Some of the lineaments belonging to the system can also be traced to the east, with some connecting NE–SW branches near the northern margin of the Carpathians.

The system of Muran lineaments in the discussed region is marked by a few short NE–SW lineaments in the eastern sectors of the Magura and Silesian units. The Myjava system, in fact one of the most prominent systems in the Carpathians, in the study area can be traced along the Nowy Sącz Basin, continuing to the north where there is a series of short lines parallel to the zone lineaments. The network interconnectivity increases in this area. The lineaments there lie in an extension of the Carpathian Shear Corridor, a large-scale strike–slip zone between Vienna and the High Tatra Mts. (Marko et al., 2017). Although the Štitnik system is unclear, some parallel or subparallel lineaments can be assigned to this zone. The Przemyśl lineament zone is identified as a set of long lineaments in the easternmost parts of the area, where the main features of NE–SW are possibly interconnected by shorter N–S lines, forming an interconnected, blocky, two-set system.

Another important deep-rooted linear structure, confirmed by a negative gravimetric anomaly is the Pericarpathian line, which runs along the Nowy Sącz–Nowy Targ–Kysucké Nové Mesto line (Zuchiewicz, 1984; Sikora, 1976), which runs similarly to the Myjava structure. The Kraków–Prešov lineament, which is an extension of the Kraków–Lubliniec fault zone and marks the border between the Małopolska and Brunovistulicum blocks of the basement (Żaba, 1999; Zuchiewicz, 1984). A system of lineaments is clearly visible along this line, mainly in the Magura Nappe; however, parallel photolineaments were marked even longer to the north (Bażyński et al., 1986).

These systems can be arranged in two sets: NNW, NW–SSE, SE striking (Central Slovakia, Skawa, Kraków–Presov and Štitnik); and NE–SE (Myjava and Pericarpathian, Muran and Przemyśl). That implies some points of system intersection, and in the area analysed such a place is in the Nowy Sącz region. This place is characterised

by higher interconnection factors (Fig. 9), in relation to the surrounding area. Moreover, in terms of geomorphology, this is an intramountainous basin, being the only location where deposits are observed in the Magura Nappe Neogene.

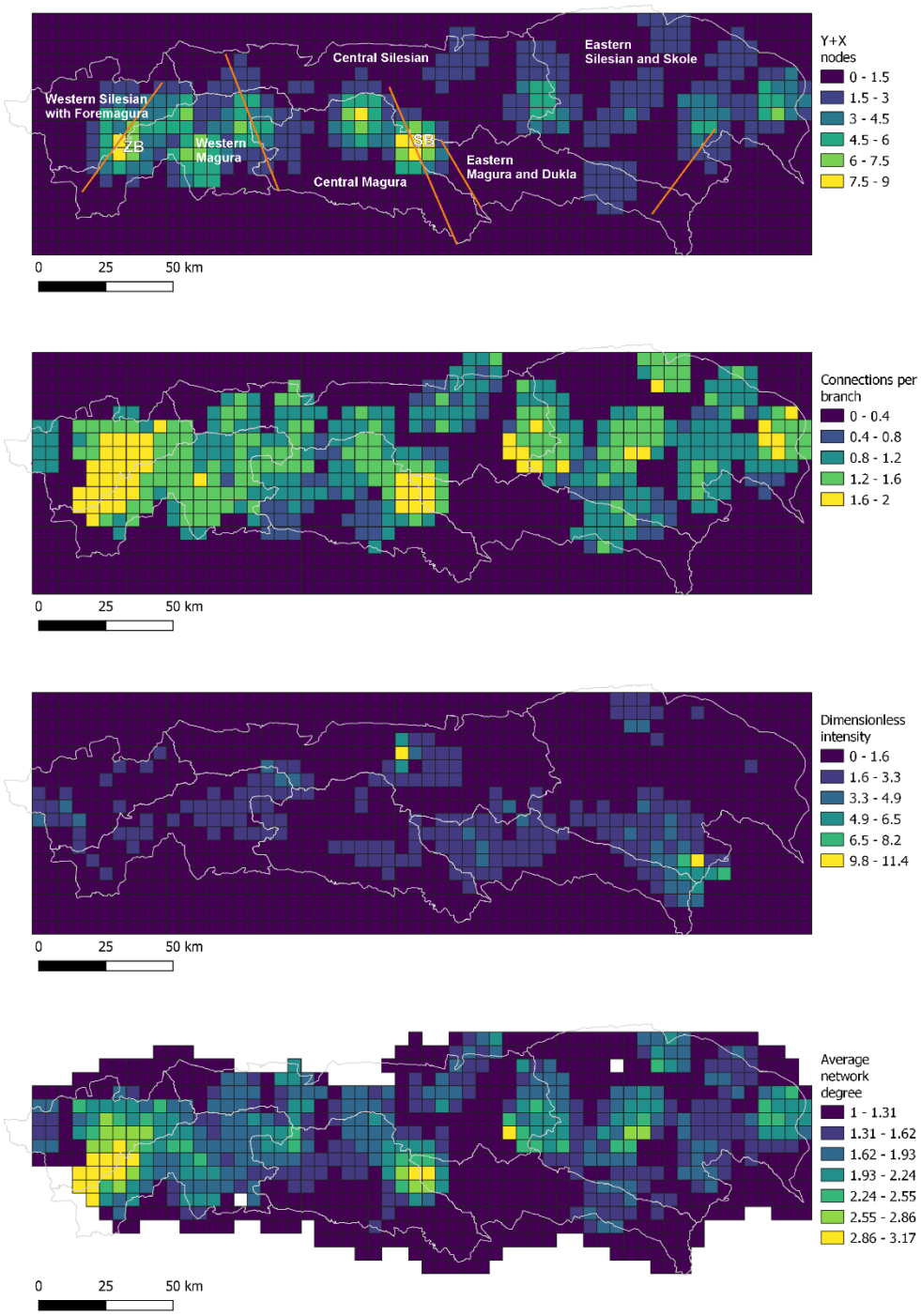

Fig. 9. Topological parameters of the lineament network, from up to down: connecting nodes number, connections per branch number, dimensionless intensity factor, and average network degree. ZB – Żywiec Basin (Żywiec tectonic window), SB – Nowy Sącz Basin, lines on X-Y nodes map are main faults.

The Central Slovakian system strikes along the east border of the Żywiec Basin and Żywiec tectonic window, where the Subsilesian Nappe is exposed. We also marked a major lineament there, which is not present on the photolineament map (Bażyński et al., 1986) or the database of the Western Carpathian Geological Map (Lexa et al., 2000). The lineament (in the central part, the Soła River Valley) cuts the Magura Nappe, the Foremagura zone with Magura overthrust and the Silesian Nappe. This structure is one of the edges of the rhomboidal block, in which the Żywiec Basin has been developed. The generally increased degree of network interconnection (Fig. 10) and the intensity of the network in this area can be an effect of the interaction between the central Slovakian system with the Soła lineament and all the lowered block edges.

The cross-cutting relations of the Myjava lineament and the Štitnik lineament, whose continuation can be the Dunajec fault system, are reflected in the bimodality of lineaments. The dominating maximum in the central Magura sector, at approximately 120°, is similar to the Štitnik lineament; however, the Myjava lineament is reflected there by just a few dominating lineaments, which are relatively long. Moreover, the Pericarpathian lineaments are also known in this region. This structure, reflected in the sedimentary cover as the Dunajec fault zone, is also confirmed by a negative gravimetric anomaly (Zuchiewicz, 1984; Sikora, 1976). Another deep structure cutting this area is the Kraków–Prešov fault, which is an extension of the Kraków–Lubliniec fault zone under the Carpathians active to the Quternary (Żaba, 1999). All these deep cross-cutting features result in an increased degree of the network connectivity observed on the surface. Then, the blocky structure allowed the formation of an intramountain basin, filled with Neogene sediments.

Topological analysis also suggests that the well-known Skawa fault zone (Zuchiewicz et al., 2009; Unrug, 1980) is in fact the western-most part of the wider zone of increased network interconnectivity, extending ca. 10–20 km to the west of the Raba River. The final interpretation of correlation of lineaments increased interconnectivity areas with tectonic structures of the area is shown on the Fig. 10.

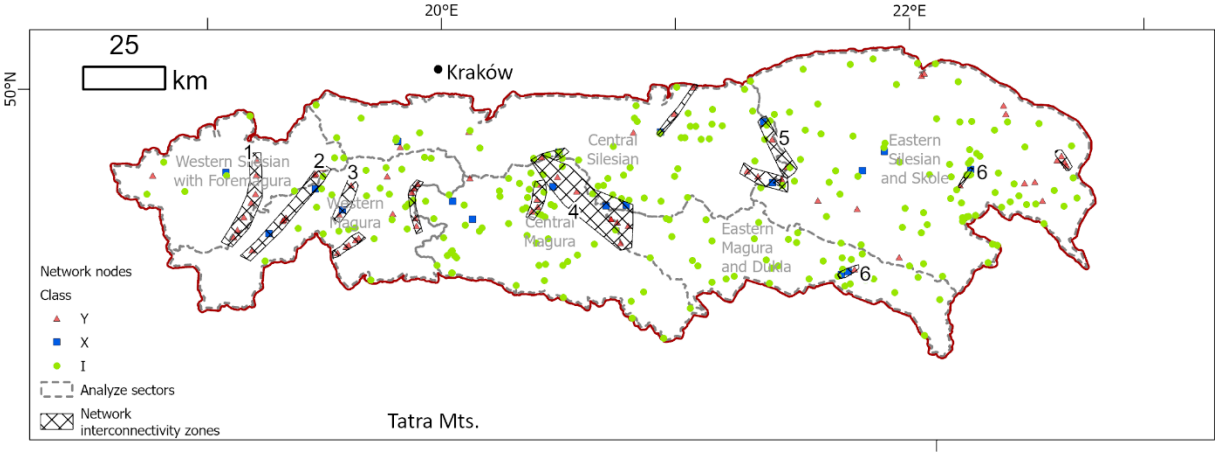

Fig. 10. Network nodes and zones of interconnectivity and their interpretation in context of Outer Carpathians Nappes (surface) and basement (deep) tectonics. 1 – Soła fault zone (surface), Central Slovakia lineament (deep), 2 – fault system along Sopotnia Valley, 3 – Skawa fault zone (surface), 4 – Nowy Sącz Basin (surface), Kraków – Prešov, Myjava and Štitnik lineaments (deep), 5 – faults along Wisłoka Valley (surface), 6 – Muran lineament (deep).

8. The other aspect of the fault system of the Carpathians is occurrence and migration of the mineral waters. The area to the south of the Nowy Sącz there is a well-known region of CO_2-rich mineral

waters occurrence with renowned spa sites. These waters are associated with fault zones, often the deep one, penetratiting to the crystalline basement of the Carpathians (Oszczypko and Zuber, 2002; Zuber and Chowaniec, 2009; Ciężkowski et al., 2010). Its noteworthy, that this region is located on the crossing of two major deep-rooted fault zones: Štitnik lineament and Myjava lineament (Fig. 8). Similarly, the deep faults can be patch of migration of hydrocarbons, especially if source rocks are related to the platform cover of Brunovistulicum and Małopolska Massif lying under the Carpathians. In fact, some of the Polish Carpathian gas deposits are related to the Mesozoic-Palaeozoic basement (Kotarba and Koltun, 2006). Thus, the analyse of the fault systems and their interconnectivity has the potential in study of both, hydrocarbon and hydrogeological systems.Conclusions

The proposed data source and analysis method are complementary with other lineament analysis from the study area. The observed azimuths are in general concordant with the photolineament network; however, there are some structures that are not confirmed by DEM interpretation. The relationship between the DEM-interpreted data and geologically confirmed faults shows the usefulness of DEM as a data source in fault detection.

The dominating directions of the network are typical for the Western Carpathians, with a clear increase of the NE striking features proportion towards the east.

The topological properties of the lineament network in the Western Carpathians show E–W trends, but no clear S–N (perpendicular to the tectonic units) trends. This justifies the proposed subdivision of the Carpathians in the western, central and eastern sectors in addition to the tectono-facial subdivision. The eastern sectors are dominated by NE–SW trends and low interconnectivity, while the central and western sectors are more interconnected and characterised by cross-cutting relationships of two main lineament directions. The degree of network interconnectivity increases in areas with a lower morphology (intramountainous basins): the Żywiec Basin and Nowy Sącz Basin.

The geometry of the network, in general, reflects a system of deep-rooted lineaments. The cross-cutting area of the main deep lineaments is reflected in stronger network interconnectivity in the Nowy Sącz area.

CrediT authorship contribution statement: Maciej Kania: Conceptualization, Methodology, Formal analysis, Investigation, Writing – original draft, Visualization. Mateusz Szczęch: Investigation, Writing – review & editing, Visualization.

Declaration of competing interest: The authors declare that they have no known competing financial interests or personal relationships that could have appeared to influence the work reported in this paper

Acknowledgements: The research was financed from funds of the Jagiellonian University Institute of Geological Sciences. Proofreading of this publication has been supported by a grant from the Priority Research Area (Digiworld) under the Strategic Programme Excellence Initiative at Jagiellonian University. The authors would like to thank both referees, Prof. Fabrizio Balsamo and Prof. Jan Golonka for their helpful comments improving a quality of the paper.

References

Baas, J. H.: EZ-ROSE: a computer program for equal-area circular histograms and statistical analysis of two-dimensional vectorial data, Computers & Geosciences, 26, 153–166, https://doi.org/10.1016/S0098-3004(99)00072-2, 2000.

Bażyński, J., Doktór, S., and Graniczny, M.: Mapa fotogeologiczna Polski w skali 1:1 000 000, 1986.

Burtan, J.: Detailed Geological Map of Poland, 1:50 000 scale, Mszana Dolna sheet. Wydawnictwa Geologiczne, Warszawa, 1974.

Chodyń, R.: Zastosowanie cyfrowego modelu terenu (DEM) w badaniach geologicznych na przykładzie obszaru między Dobczycami a Mszaną Dolną (polskie Karpaty zewnętrzne), Przegląd Geologiczny, 52, 315–320, 2004.

Cieszkowski, M., Golonka, J., Waśkowska-Oliwa, A., and Chrustek, M.: Budowa geologiczna rejonu Sucha Beskidzka – Świnna Poręba (polskie Karpaty fliszowe), Geologia / Akademia Górniczo-Hutnicza im. Stanisława Staszica w Krakowie, 32, 155–201, 2006.

Cieszkowski, M., Kysiak, T., Szczęch, M., and Wolska, A.: Geology of the Magura Nappe in the Osielec area with emphasis on an Eocene olistostrome with metabasite olistoliths (Outer Carpathians, Poland), Annales Societatis Geologorum Poloniae, 87, 169–182, https://doi.org/10.14241/asgp.2017.009, 2017.

Ciężkowski, W., Chowaniec, J., Górecki, W., Krawiec, A., Rajchel, L. and Zuber, A.: Mineral and thermal waters of Poland, Przegląd Geologiczny, 58, 762–773, 2010.

Danielson, J. J.: Global Multi-resolution Terrain Elevation Data 2010 (GMTED2010) Coastal Elevation Modeling View project LP DAAC View project, 2011.

Doktór, S. and Graniczny, M.: Geologiczna interpretacja zdjęć satelitarnych i radarowych wschodniej części Karpat, Kwartalnik Geologiczny, 26, 231–245, 1982.

Doktór, S. and Graniczny, M.: Fotogeologiczna analiza zdjęć satelitarnych Karpat, Kwartalnik Geologiczny, 27, 645–656, 1983.

Doktór, S., Dornic, J., Graniczny, M., and Reichwalder, P.: Structural elements of Western Carpathians and their Foredeep on the basis of satellite interpretation, Geological Quarterly, 29, 129–138, 1985.

Doktór, S., Graniczny, M., Kucharski, R., Molek, M., and Dąbrowska, B.: Wgłębna budowa geologiczna Karpat w świetle kompleksowej analizy teledetekcyjno-geofizycznej, Przegląd Geologiczny, 38, 469–475, 1990.

Doktór, S., Graniczny, M., Kowalski, Z., and Wójcik, A.: Możliwości zastosowania wyników interpretacji zdjęć radarowych do analizy tektonicznej Karpat, Przegląd Geologiczny, 50, 852–860, 2002.

Ehlen, J.: Lineation, edited by: Goudie, A. S., Encyclopedia of Geomorphology, 2, 623–624, 2004.

Golonka, J., Aleksandrowski Pawełand Aubrecht, R., Chowaniec, J., Chrustek, M., Cieszkowski, M., Florek, R., Gawęda, A., Jarosiński, M., Kępińska, B., and others: The Orava deep drilling project and post-palaeogene tectonics of the northern Carpathians, Annales Societatis Geologorum Poloniae, 75, 211–248, 2005.

Golonka, J., Waśkowska, A., and Ślączka, A.: The Western Outer Carpathians: Origin and evolution, Zeitschrift der Deutschen Gesellschaft für Geowissenschaften, 229–254, 2019.

Golonka, J., Gawęda, A., and Waśkowska, A.: Carpathians, Reference Module in Earth Systems and Environmental Sciences, in: Alderton, D. and Elias, S. A. (eds.): Encyclopedia of Geology (Second Edition), Academic Press, 372–381, https://doi.org/10.1016/b978-0-12-409548-9.12384-x, 2021.

Graniczny, M. and Mizerski, W.: Lineamenty na zdjęciach satelitarnych Polski – próba podsumowania, Przegląd Geologiczny, 51, 474–482, 2003.

Kania, M. and Szczęch, M.: Geometry and topology of tectonolineaments in the Gorce Mts. (Outer Carpathians) in Poland, J Struct Geol, 141, 104186, https://doi.org/10.1016/j.jsg.2020.104186, 2020.

Kania, M. and Szczęch, M.: Tectonic Structures Interpretation Using Airborne-Based LiDAR DEM on the Examples from the Polish Outer Carpathians, in: Atlas of Structural Geological and Geomorphological Interpretation of Remote Sensing Images, edited by: Misra, A. A. and Mukherjee, S., 157–165, 2022.

Kotarba, M.J. and Koltun, Y.V.: The Origin and habitat of hydrocarbons of the Polish and Ukrainian parts of the Carpathian Province, in: Golonka, J. and Picha, F., The Carpathians and Their Foreland: Geology and Hydrocarbon Resources: AAPG Memoir, 84, 321–368, 2006.

Książkiewicz, M.: The Tectonics of the Carpathians, in: Geology of Poland, vol. 4. Tectonics. The Alpine Tectonic Epoch, Geological Institute, Warszawa, 476–608, 1977.

Leech, D. P., Treloar, P. J., Lucas, N. S., and Grocott, J.: Landsat TM analysis of fracture patterns: A case study from the Coastal Cordillera of northern Chile, Int J Remote Sens, 24, 3709–3726, https://doi.org/10.1080/0143116031000102520, 2003.

Lexa, J., Bezák, V., Elečko, M., Mello, J., Polák, M., and Vozár, J.: Geological map of western Carpathians and adjacent areas 1:500 000, 2000.

Mahel', M.: Tectonics of the Carpathian–Balkan Regions, Explanations to the Tectonic Map of the Carpathian-Balkan Regions and Their Foreland., Štátny geologický ústav Dionýza Štúra, Bratislava, 180–197 pp., 1974.

Marko, F., Andriessen, P. A. M., Tomek, Č., Bezák, V., Fojtíková, L., Bošanský, M., Piovarči, M., and Reichwalder, P.: Carpathian Shear Corridor – A strike-slip boundary of an extruded crustal segment, Tectonophysics, 703–704, 119–134, https://doi.org/10.1016/j.tecto.2017.02.010, 2017.

Van der Meer, F. D., van der Werff, H. M. A., van Ruitenbeek, F. J. A., Hecker, C. A., Bakker, W. H., Noomen, M. F., van der Meijde, M., Carranza, E. J. M., de Smeth, J. B., and Woldai, T.: Multi- and hyperspectral geologic remote sensing: A review, https://doi.org/10.1016/j.jag.2011.08.002, 2012.

Minár, J., Bielik, M., Kováč, M., Plašienka, D., Barka, I., Stankoviansky, M., and Zeyen, H.: New morphostructural subdivision of the Western Carpathians: An approach integrating geodynamics into targeted morphometric analysis, Tectonophysics, 502, 158–174, 2011.

Motyl-Rakowska, J. and Ślączka, A.: Ważniejsze lineamenty Karpat i ich związek ze znanymi uskokami, Przegląd Geologiczny, 32, 72–77, 1984.

Mukherjee, S.: Using Graph Theory to Represent Brittle Plane Networks, 259–271, https://doi.org/10.1016/B978-0-12-814048-2.00022-3, 2019.

Nagi, R.: Introducing Esri's Next Generation Hillshade: https://www.esri.com/arcgis-blog/products/arcgis-living-atlas/imagery/introducing-esris-next-generation-hillshade/?rmedium=redirect&rsource=blogs.esri.com/esri/arcgis/2014/07/14/introducing-esris-next-generation-hillshade, last access: 1 June 2022.

Nyberg, B., Nixon, C. W., and Sanderson, D. J.: NetworkGT: A GIS tool for geometric and topological analysis of two-dimensional fracture networks, Geosphere, 14, 1618–1634, https://doi.org/10.1130/GES01595.1, 2018.

O'Leary, D. W., Friedman, J. D., and Pohn, H. A.: Lineament, linear, lineation: Some proposed new standards for old terms, Geological Society of America Bulletin1, 87, 1463–1469, 1976.

Oszczypko, N.: Late Jurassic-Miocene evolution of the Outer Carpathian fold-and-thrust belt and its foredeep basin (Western Carpathians, Poland), Geological Quarterly, 50, 169–194, 2006.

Oszczypko, N. and Zuber, A.: Geological and isotopic evidence of diagenetic waters in the Polish Flysch Carpathians. Geologica Carpathica, 53, 257–268, 2002.

Ozimkowski, W.: Lineamenty otoczenia Tatr - porównanie interpretacji DEM i MSS, Przegląd Geologiczny, 56, 1099–1102, 2008.

Plašienka, D.: Continuity and episodicity in the early Alpine tectonic evolution of the Western Carpathians: How large-scale processes are expressed by the orogenic architecture and rock record data, Tectonics, 37, 2029–2079, 2018.

Procter, A. and Sanderson, D. J.: Spatial and layer-controlled variability in fracture networks, J Struct Geol, 108, 52–65, https://doi.org/10.1016/j.jsg.2017.07.008, 2018.

Sanderson, D. J. and Nixon, C. W.: The use of topology in fracture network characterization, J Struct Geol, 72, 55–66, https://doi.org/10.1016/j.jsg.2015.01.005, 2015.

Sanderson, D. J., Peacock, D. C. P., Nixon, C. W., and Rotevatn, A.: Graph theory and the analysis of fracture networks, J Struct Geol, 14th April, https://doi.org/10.1016/j.jsg.2018.04.011, 2018.

Scheiber, T., Fredin, O., Viola, G., Jarna, A., Gasser, D., and Łapińska-Viola, R.: Manual extraction of bedrock lineaments from high-resolution LiDAR data: methodological bias and human perception, 137, 362–372, https://doi.org/10.1080/11035897.2015.1085434, 2015.

Sikora, W.: On lineaments found in the Carpathians, Rocznik Polskiego Towarzystwa Geologicznego, 46, 3–37, 1976.

Ślączka, A., Kruglov, S., Golonka, J., Oszczypko, N., and Popadyuk, I.: Geology and hydrocarbon resources of the Outer Carpathians, Poland, Slovakia, and Ukraine: general geology, in: Golonka, J. and Picha, F., The Carpathians and Their Foreland: Geology and Hydrocarbon Resources: AAPG Memoir, 84, 221–258, 2006.

Solon, J., Borzyszkowski, J., Małgorzata Bidłasik, Richling, A., Badora, K., Balon, J., Brzezińska-Wójcik, T., Chabudziński, Ł., Dobrowolski, R., Grzegorczyk, I., Jodłowski, M., Kistowski, M., Kot, R., Krąż, P., Lechnio, J., Macias, A., Majchrowska, A., Malinowska, E., Migoń, P., Myga-Piątek, U., Nita, J., Papińska, E., Rodzik, J., Strzyż, M., Terpiłowski, S., Ziaja, W., and Paul, J.: Physico-geographical mesoregions of Poland: verification and adjustment of boundaries on the basis of contemporary spatial data, Geographia Polonica, 91, 143–170, https://doi.org/10.7163/GPol.0115, 2018.

Szczęch, M. and Cieszkowski, M.: Geology of the Magura Nappe, south-western Gorce Mountains (Outer Carpathians, Poland), Journal of Maps, 17, 453–464, https://doi.org/10.1080/17445647.2021.1950579, 2021.

Teisseyre, W.: O związku w budowie tektonicznej Karpat i ich przedmurza, Kosmos, 32, 393–402, 1907.

Statistics (scipy.stats) — SciPy v1.9.3 Manual: https://docs.scipy.org/doc/scipy/tutorial/stats.html, last access: 8 November 2022.

Thiele, S. T., Jessell, M. W., Lindsay, M., Ogarko, V., Wellmann, J. F., and Pakyuz-Charrier, E.: The topology of geology 1: Topological analysis, Journal of Structural Geology, 91, 27–38, https://doi.org/10.1016/J.JSG.2016.08.009, 2016.

Unrug, R.: Tectonic rotation of flysch nappes in the Polish Outer Carpathians, Rocznik Polskiego Towarzystwa Geologicznego, 50, 27–39, 1980.

Valentini, L., Perugini, D., and Poli, G.: The "small-world" topology of rock fracture networks, Physica A: Statistical Mechanics and its Applications, 377, 323–328, https://doi.org/10.1016/j.physa.2006.11.025, 2007.

Wójcik, A., Czerwiec, J., and Krawczyk, M.: Szczegółowa Mapa Geologiczna Polski 1:50 000. arkusz Limanowa, 2009.

Yang, L., Meng, X., and Zhang, X.: SRTM DEM and its application advances, https://doi.org/10.1080/01431161003786016, 2011.

Zuber, A. and Chowaniec, J.: Diagenetic and other highly mineralized waters in the Polish Carpathians, Applied Geochemistry, 24, 1889–1900, 2009.

Zuchiewicz, W.: The late Neogene - Quaternary tectonic mobility of the Polish West Carpathians - a case study of the Dunajec drainage basin, Annales Societatis Geologorum Poloniae, 54, 133–189, 1984.

Zuchiewicz, W., Tokarski, A. K., Świerczewska, A., and Cuong, N. Q.: Neotectonic Activity of the Skawa River Fault Zone (Outer Carpathians, Poland), Annales Societatis Geologorum Poloniae, 79, 67–93, 2009.

Żaba, J.: Ewolucja strukturalna utworów dolnopaleozoicznych w strefie granicznej bloków górnośląskiego i małopolskiego, Prace Państwowego Instytutu Geologicznego, 166, 1–162, 1999.

Żelaźniewicz, A., Aleksandrowski, P., Buła, Z., Kornkowski, P. H., Konon, A., Oszczypko, N., Ślączka, A., Żaba, J. and Żytko, K.: Regionalizacja Tektoniczna Polski. Komitet Nauk Geologicznych PAN, Wrocław, 1–60 pp., 2011.